Zeitschrift: IABSE reports of the working commissions = Rapports des commissions de travail AIPC = IVBH Berichte der Arbeitskommissionen

Band: 29 (1979)

Artikel: Plastic solutions for reinforced concrete beams in shear

Autor: Jensen, J.F.

DOI: https://doi.org/10.5169/seals-23536

II

Plastic Solutions for Reinforced Concrete Beams in Shear

Solutions plastiques pour des poutres en béton armé soumises à un effort tranchant

Plastizitätstheoretische Lösungen für schubbeanspruchte Stahlbetonbalken

J.F. JENSEN
Civil Engineer, M.Sci.Eng.
Technical University of Denmark
Lyngby, Denmark

SUMMARY
The paper treats reinforced concrete beams in shear by means of the theory of plasticity. Disregarding the tensile strength of the concrete, exact solutions are found for some common cases of beams and loading, and comparison is made with test results. Furthermore, an upper-bound analysis is carried out to investigate the influence of the tensile strength of the concrete in beams without shear reinforcement.

RESUME
La théorie de la plasticité est appliquée pour l'analyse des poutres en béton armé soumises à un effort tranchant. La résistance à la traction du béton étant supposée négligeable, quelques solutions complètes sont établies et des comparaisons avec des résultats expérimentaux sont faites. L'influence de la résistance à la traction du béton sur la charge ultime de poutres sans armature de cisaillement est examinée par la méthode cinématique.

ZUSAMMENFASSUNG
Durch Querkraft beanspruchte Stahlbetonbalken werden mit der Plastizitätstheorie behandelt. Unter der Annahme einer verschwindenden Betonzugfestigkeit werden vollständige Lösungen für einige übliche Fälle angegeben, und Vergleiche mit Versuchsergebnissen werden durchgeführt. Der Einfluss der Betonzugfestigkeit auf die Traglast von Balken ohne Schubbewehrung wird mit der kinematischen Methode untersucht.

1. INTRODUCTION

This paper presents briefly a number of plastic solutions for determination of the shear strength of reinforced concrete beams. For the detailed examination, the reader is referred to [4].

2. BASIC ASSUMPTIONS

The solutions presented are based on the following assumptions:
- The concrete is a rigid, perfectly plastic material with Coulombs modified failure hypothesis as its yield criterion. The angle of friction is φ, the uniaxial compression strength is f_c^*, and the tensile strength $f_t^* = \rho f_c^*$. The deformations are governed by the normality condition.
- The reinforcing steel is rigid, perfectly plastic, and can only resist forces in its longitudinal direction. The magnitude of the yield stress is the same for tension as for compression.
- The stress field in the beam is plane.

3. SOME EXACT SOLUTIONS

In the solutions in this section it is assumed that the concrete has no tensile strength, i.e., that $f_t^* = 0$. Regarding the consequences of this assumption, see section 4.

3.1 Stringer beam with shear reinforcement - concentrated load.

Plastic solutions for this type of beam and load, see fig. 1, have been known for some years, [1] and [2]. However, none of these works give coinciding upper-bound and lower-bound solutions for beams with very little shear reinforcement, which is a somewhat unsatisfactory state of affairs. It will be shown here how the desired coincidence can be obtained by quite a simple alteration of the stress distribution on which lower-bound solutions known so far are based.

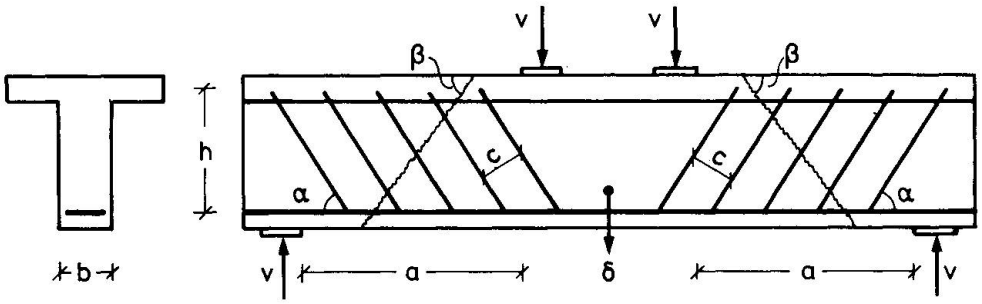

Fig. 1. Beam under consideration, showing failure mechanism.

In the following, the compression zone and the tensile reinforcement are idealized as stringers, and these are at the same time assumed to be sufficiently strong to resist the stringer forces occurring.

Furthermore, the stirrups, which are all inclined at the angle α with the beam axis, are assumed to be placed so closely together that the stirrup forces can be substituted by a uniformly distributed equivalent stirrup stress.

Let us now consider the part of the beam located between the loading plate and the support, with the distribution of the concrete stresses in the beam web shown in fig. 2. Here, the best lower-bound is obtained by optimizing the angle θ, putting

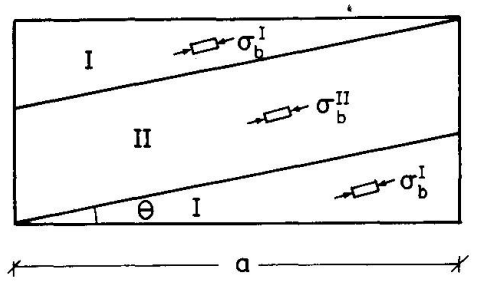

Fig. 2. Stress field in concrete with low degree of reinforcement.

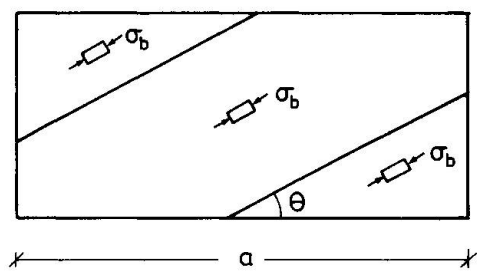

Fig. 3. Stress field in concrete with high degree of reinforcement.

$\sigma_b^{II} = f_c^*$ and assuming yielding of the shear reinforcement. The solution found in this way is valid as long as σ_b^I together with the equivalent stirrup stress fulfil the boundary conditions along the stringers without exeeding the uniaxial compression strength of the concrete, f_c^*. With the stress distribution applied, this is possible as long as

$$\psi \le \psi' = \frac{\sqrt{1+(\frac{a}{h})^2} - \frac{a}{h}}{2\sin^2\alpha\sqrt{1+(\frac{a}{h})^2}} \qquad \psi = \frac{A_s f_{ys}}{b\,c\,f_c^*} \tag{3.1}$$

Here, we have introduced the mechanical degree of shear reinforcement, ψ. A_s denotes the stirrup area crossing the concrete area $b \cdot c$, c is the spacing between the stirrups measured at right angles to these, and finally f_{ys} is the yield stress of the stirrup reinforcement.

In case of larger degrees of shear reinforcement than given by (3.1), the stress distribution from fig. 2 must be replaced by that shown in fig. 3. Here, we put $\sigma_b = f_c^*$, and for a given equivalent stirrup stress, the angle θ is determined such that the boundary conditions slong the stringers is fulfilled in all zones shown. The equivalent stirrup stress is then optimized, leading to yielding of the shear reinforcement as long as

$$\psi \le \psi'' = \frac{1+\cos\alpha}{2\sin^2\alpha} \tag{3.2}$$

while the best lower-bound is obtained without yielding of the shear reinforcement, when $\psi \ge \psi''$.

The complete result of the lower-bound solution can be written as follows:

$$\frac{\tau}{f_c^*} = \frac{V}{b\,h\,f_c^*} = \tfrac{1}{2}\left(\sqrt{1+(\tfrac{a}{h})^2} - \tfrac{a}{h}\right) + \psi\sin^2\alpha\left(\tfrac{a}{h} + \cot\alpha\right), \quad \psi \le \psi' \tag{3.3}$$

$$\frac{\tau}{f_c^*} = \sqrt{\psi\sin^2\alpha(1-\psi\sin^2\alpha)} + \psi\sin\alpha\cos\alpha, \quad \psi' \le \psi \le \psi'' \tag{3.4}$$

$$\frac{\tau}{f_c^*} = \tfrac{1}{2}\cot\frac{\alpha}{2}, \quad \psi'' \le \psi \tag{3.5}$$

The solution determined by means of (3.3) - (3.5) is exact, because an upper-bound solution derived on the basis of the failure mechanism from fig. 1 gives the same carrying capacity when the angle β is optimized.

Fig. 4 shows the results of 84 shear tests on simple T-beams with vertical stirrups, carried out in the years 1967 to 1975 at the Structural Research Laboratory of the Technical University of Denmark, compared with the theory. In the diagram, an empirical expression from [1] is used for determining the apparent strength of the concrete in the beam web on the basis of a given cylinder compression strength, valid for stringer beams with shear reinforcement:

$$f_c^* = (0.8 - \frac{f_c}{200}) \cdot f_c \qquad (3.6)$$

In (3.6), both f_c^* and f_c are measured in MPa, f_c denoting the cylinder strength.

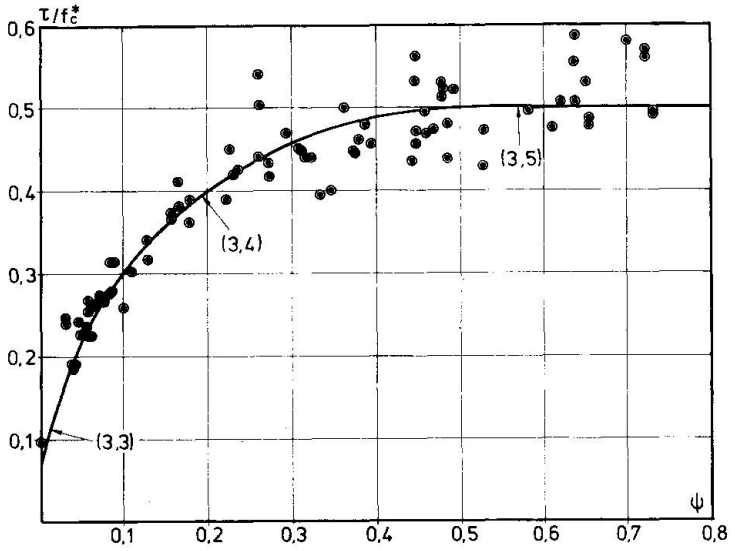

Fig. 4.
Comparison of the theory and the results of tests.

3.2 Rectangular beam without shear reinforcement - uniformly distributed load.

We now consider a simply supported beam with the free span 2a, see fig. 5. It is assumed that the force, T, in the tensile reinforcement can be transmitted to the concrete by the part of the beam lying behind the support, as shown, in principle, in the figure.

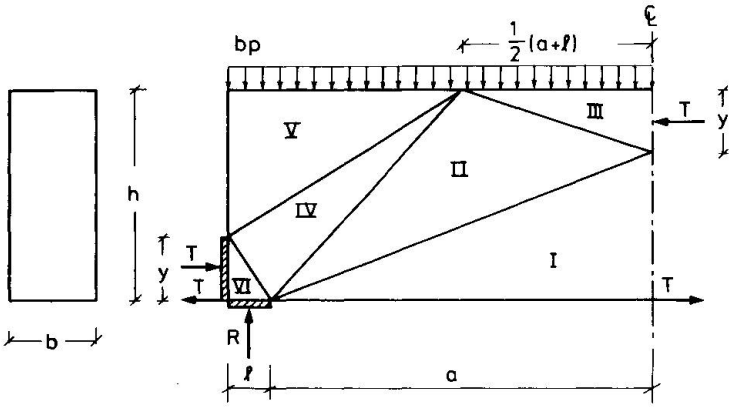

Fig. 5. Beam under consideration showing adopted division of concrete into zones with homogeneous stress fields.

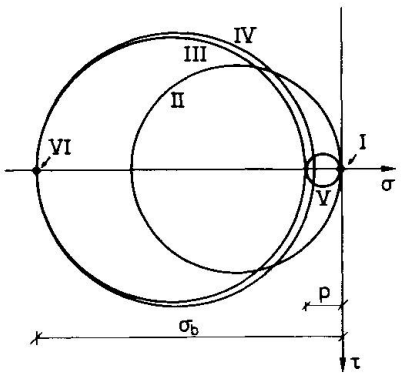

Fig. 6. Mohr's circles for the stress fields in the zones from fig. 5.

The concrete is divided into zones with homogeneous stress fields, as shown in fig. 5. The stress fields are illustrated by means of the Mohr's circles in fig. 6. As seen, the length ℓ is determined such that hydrostatic pressure is obtained in zone VI. No tensile stresses occur in any part of the concrete, and in the best solution, the largest compression stress, σ_b, is obtained simultaneously in zones III, IV and VI. We put $\sigma_b = f_c^*$, giving the magnitude of y, and the solution then becomes:

$$\frac{\tau}{f_c^*} = \frac{p\,a}{h\,f_c^*} = \frac{2\Phi(1-\Phi)\frac{a}{h}}{(\frac{a}{h})^2 + 2\Phi(1-\Phi)} \quad , \quad \Phi = \frac{A_\ell\, f_{y\ell}}{b\,h\,f_c^*} \leq \tfrac{1}{2} \qquad (3.7)$$

$$\frac{\tau}{f_c^*} = \frac{\frac{a}{h}}{2\left(\frac{a}{h}\right)^2 + 1} \qquad \Phi \geq \tfrac{1}{2} \qquad (3.8)$$

where we have introduced the mechanical degree of longitudinal reinforcement, Φ. A_ℓ is the cross-sectional area of the reinforcement, and $f_{y\ell}$ is the yield stress of the same. In opposition to (3.7), no yielding of the reinforcement occur corresponding to (3.8).

The solution given by (3.7) and (3.8) is exact, since an upper-bound solution based on the failure mechanism from fig. 7 leads to the same carrying capacity. The points A and B act as hinges, and part I rotates an angle θ about the point A. Part II's displacement is a pure translation.

Fig. 8 shows a comparison of the results obtained in theory and those obtained from tests for a narrow interval of degrees of reinforcement. A detailed analysis of the test results versus theory has not yet been performed. Therefore, since the apparent concrete strength will presumably vary in relation to the cylinder compression strength, analogously to (3.6), we have chosen only to consider a number of tests with concrete strengths that do not vary too much in relation to each other. We have then tentatively put $f_c^* = 0.65\ f_c$.

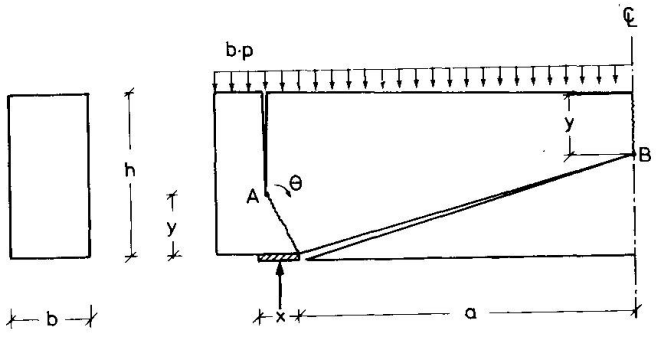

Fig. 7. Failure mechanism used.

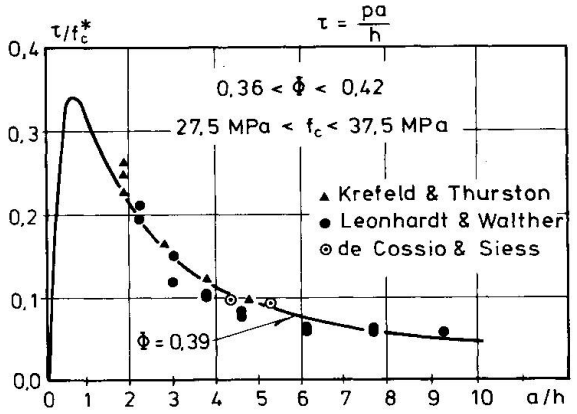

Fig. 8. Comparison with tests from the literature.

With regard to the type of load and beam considered here, it is also interesting to compare the carrying capcitites measured in tests reported in the literature with the flexural strength determined in accordance with the CEB-FIP Model Code. In a comparison of this nature reported in [1] and [3] for a total of 115 tests, the average value of the ratio between the two carrying capacities is found to be 1.00, with a coefficient of variation of 15.2%. Thus, apart from ensuring a ductile failure, only little can generally be gained by reinforcing with stirrups.

3.3 Rectangular beam without shear reinforcement - combined central, normal force and concentrated load.

For derivation of the lower-bound solution, use is made of the stress distribution shown in fig. 9. Forces in the tensile reinforcement are assumed to be transmitted to the concrete behind the support, as in case of the beam in section 3.2.

The corresponding upper-bound is derived on the basis of a failure mechanism analogous to that shown in fig. 7., see fig. 10. The best solution is found by optimizing x, y_1 and y_2.

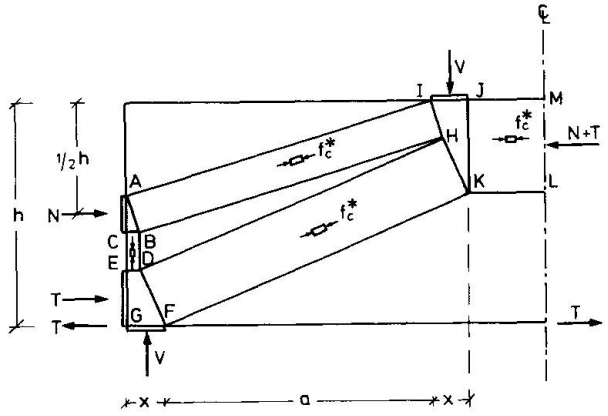

Fig. 9. Stress distribution for use in lower-bound solution.

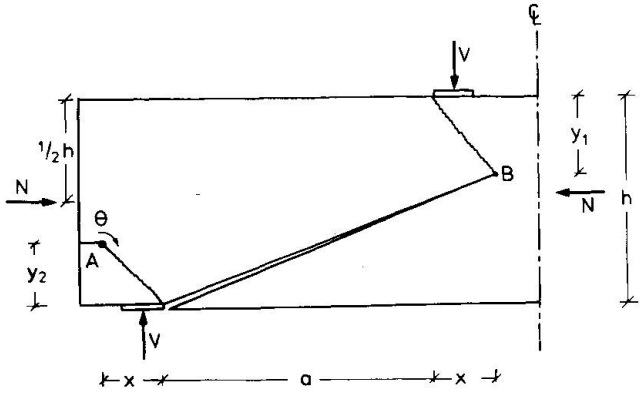

Fig. 10. Sketch showing failure mechanism used.

Both the lower-bound and the upper-bound solution leads to the carrying capacities:

$$\frac{\tau}{f_c^*} = \frac{V}{b\,h\,f_c^*} = \tfrac{1}{2}\left(\sqrt{2\pi(1-\pi-2\Phi)+4\Phi(1-\Phi)+\left(\frac{a}{h}\right)^2}-\left(\frac{a}{h}\right)\right), \quad 0 \le \pi \le 1-2\Phi \qquad (3.9)$$

$$\frac{\tau}{f_c^*} = \tfrac{1}{2}\left(\sqrt{1-\pi^2+\left(\frac{a}{h}\right)^2}-\frac{a}{h}\right), \quad 1-2\Phi \le \pi \le 1 \qquad (3.10)$$

where we have introduced the dimensionless parameter, π, by $N = \pi\, b\, h\, f_c^*$, and the degree of longitudinal reinforcement, Φ, from (3.7). Only corresponding to (3.9), yielding of the reinforcement is obtained.

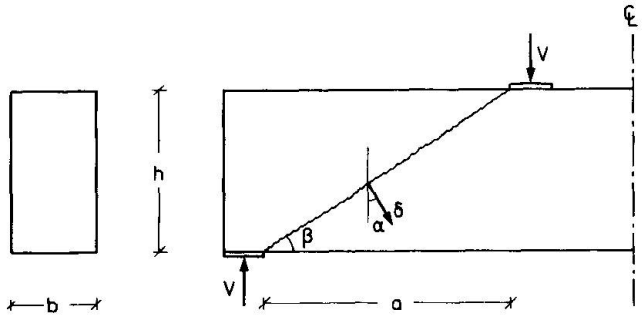

Fig. 11. Alternative failure mechanism for $\pi = 0$.

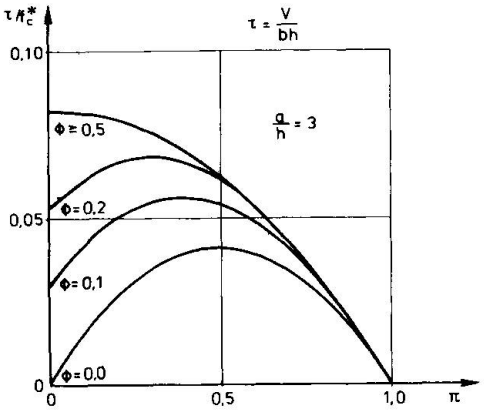

Fig. 12. Variation of carrying capacity with Φ and π.

Now, compare the failure mechanism from fig. 10 with that from fig. 11. When the beam is not subjected to a normal force, the mechanism from fig. 11 leads when α is optimized to the same carrying capacity as given by (3.9) - (3.10) for $\pi = 0$. Here α denotes the angle between the vertical and the relative displacement, δ, between zones I and II. In this case, the solution is well known, and comparisons with tests have previously been performed, cf. [1] and [3].

For $\pi \neq 0$, the solution has not yet been verified by tests, so in fig. 12 only the theoretical relationship between the carrying capacity and a couple of the main parametres is shown. The variation with the relative shear span, $\frac{a}{h}$, is analogous to that shown in fig. 14 for $\rho = 0$.

4. UPPER-BOUND ANALYSIS OF THE EFFECT OF TENSILE STRENGTH

In beams provided with shear reinfrocement, the concrete in the beam web will be completely cracked all the way through before failure occurs, so the concrete cannot be assumed to have any tensile strength in a determination of the carrying capacity. Therefore, in this section only beams without shear reinforcement will be considered, since the cracking here will be less pronounced, which means that the concrete can reasonably be assumed to have a certain, although minimum, tensile strength.

4.1 Rectangular beam without shear reinforcement - concentrated load.

The failure mechanism shown in fig. 13 is chosen as the basis for the upper-bound solution. At failure, the middle part of the beam undergoes the relative displacement, δ, vertically downwards in relation to the parts of the beam over the supports, since we will only consider beams with such strong longitudinal reinforcement that yielding will not occur in this. The failure line adopted is straight in all cases, which is also shown by variational analysis to be the optimum form. The best upper-bound solution is obtained by optimizing the angle β.

The solution arrived at is illustrated in fig. 14, where it should be noted that the hereby calculated shear capacity becomes independent of the shear span when this exeeds a certain limit, even though the concrete is only assumed to have a rather low tensile strength. This indicates, as is well known, that if the shear span is sufficiently long, then another failure mechanism, the flexural failure, must be more dangerous than the shear failure.

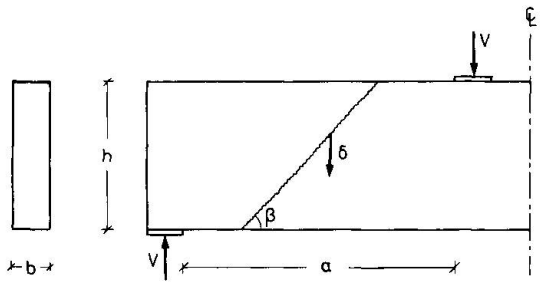

Fig. 13. Failure mechanism.

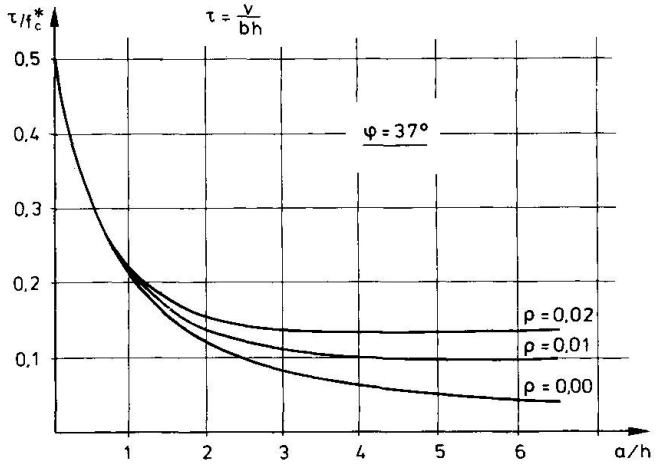

Fig. 14. Variation of shear capacity with ρ and $\frac{a}{h}$. $f_t^* = \rho f_c^*$.

If this had been a stringer beam with sufficiently strong stringers, the solution illustrated in fig. 14 would be exact, since in this case a corresponding lower-bound solution is found in [4].

4.2 Rectangular beam without shear reinforcement - uniformly distributed load.

Generalizing the failure mechanism from fig. 7 to that shown in fig. 15 for a beam with such strong longitudinal reinforcement that yielding of this will not occur, we find by optimation that $y = \frac{1}{2}h$ and $x_1 = 0$. The best value for x_2 and d for use in the following has been calculated numerically. The results are shown in fig. 16 and 17.

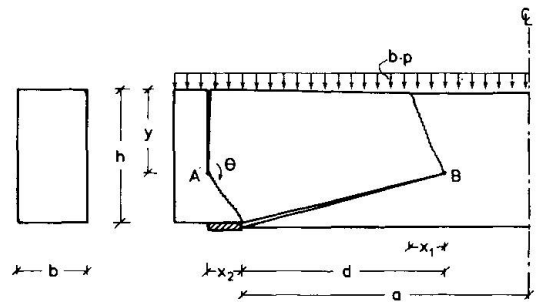

Fig. 15. Failure mechanism.

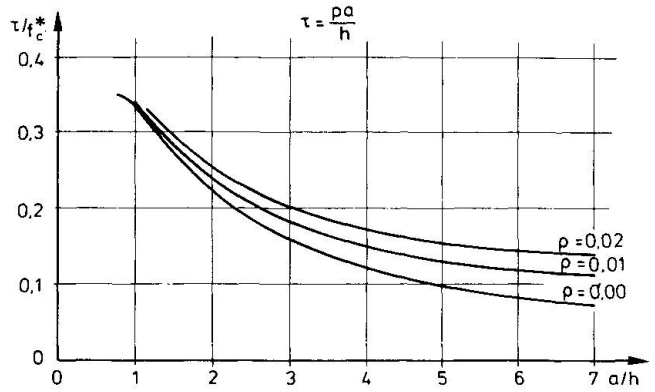

Fig. 16. Variation of carrying capacity with ρ and $\frac{a}{h}$.

Fig. 17. Example of geometry of failure pattern at $\frac{a}{h} = 3$.

Note from fig. 17 how the compression failures in the top of the beam move out towards the supports, when the tensile strength is taken into account.

REFERENCES

[1] Nielsen, M.P., M.W. Bræstrup, B.C. Jensen and F. Bach:"Concrete Plasticity". Dansk Selskab for Bygningsstatik. Special Publication. Copenhagen, 1978.

[2] Thürlimann, B.:"Plastic Analysis of Reinforced Concrete Beams". IABSE Colloquium, Copenhagen, 1979. Introductory Report, pp. 71-90.

[3] Roikjær, M., C. Pedersen, M.W. Bræstrup, M.P. Nielsen og F. Bach: "Bestemmelse af ikke-forskydningsarmerede bjælkers forskydningsbæreevne". Rapport Nr. I 62, Afdelingen for Bærende Konstruktioner, Danmarks tekniske Højskole, 1978.

[4] Jensen, J.F., M.W. Bræstrup, F. Bach og M.P. Nielsen:"Nogle plasticitetsteoretiske bjælkeløsninger". Rapport Nr. R 101, Afdelingen for Bærende Konstruktioner, Danmarks tekniske Højskole, 1978.